Jurnal Presipitasi
Media Komunikasi dan Pengembangan Teknik Lingkungan
e-ISSN : 2550-0023

Vol 18, No 1, 2021, 88-98
Article available at homepage presipitasi

Research article

Decontamination of Mercury from Mined Soil using Magnetite Functionalized Quaternary Ammonium Silica (Fe3O4/SAK)

Ngatijo[1]*, Defia Indah Permatasari[1], Faizar Farid[1], Restina Bemis[1], Heriyanti[1], Rahmat Basuki[2], Yudha Gusti Wibowo[3]

[1] Program of Chemistry, Fakulty of Science and Technology, Universitas Jambi
[2] Department of Chemistry, Faculty of Military Mathematics and Natural Sciences, Universitas Pertahanan RI
[3] Department of Environmental Engineering, Universitas Diponegoro, Semarang, Indonesia
*Correspondence email: tijo52@yahoo.co.id

Abstract

Artisanal small-scale gold mining (ASCGM) has caused mercury contamination. However, efforts to decontaminate mercury from the ex-mining soils are still rare. This study aims to synthesize quaternary ammonium silica functionalized magnetite (Fe_3O_4/SAK) as a low price, highly available, and quickly separated adsorbent for mercury decontamination from ex-mining soils samples. The synthesis of Fe_3O_4/SAK and the mercury decontamination process was carried out by the co-precipitation and batch type reactor procedure, respectively. The Fourier Transform-Infra Red (FT-IR) characterization of synthesized Fe_3O_4/SAK informed the appearance of siloxane, silanol, methyl, methylene, and Fe-O functional groups. Crystal analysis by X-Ray Diffraction (XRD) showed that the typical peaks of SiO_2 and Fe_3O_4 were emerged at 2θ 22.8° and 35.52°, respectively. Morphological studies and elemental analysis using Scanning Electron Microscopy-Energy Dispersive X-Ray (SEM-EDX) indicated the successful functionalization Fe_3O_4 by SAK in the transformation of surface morphology and composition of the main elements, namely C, O, Si, and Fe. The results of characterization using Surface Area Analyzer (SAA) showed that the surface area and pore diameters were 224.98 m^2/g and 36.149-38.70 Å, respectively. The optimum results for adsorbing Hg_2^{2+} metal ions were obtained at pH 4.0, and the adsorbent mass was 0.1 g. The Fe_3O_4/SAK has been proven to be an easily separable adsorbent after the mercury decontamination process in ex-mining soil samples with an adsorption efficiency of 43.36% (0.722 mg/g).

Keywords: mercury decontamination, former mining soil, magnetite functionalized quaternary ammonium silica.

1. Introduction

Mining is one of the mainstay industries for earning foreign exchange in the context of sustainable development. Mining activities are part of all phases of activities, including general investigation, exploration, feasibility studies, mining construction, processing and refining, transportation, and sale of minerals and coal (Winarno *et al.*, 2020). Gold is a mineral that is widely mined because it has a high and stable price. A large number of gold deposits in various parts of Indonesia opens up opportunities for people to carry out gold mining. The impact of mining activities can be positive in areas for mining entrepreneurs. However, gold mining activities also negatively impact if the local community does not permit a government agency following the prevailing laws and regulations. Thus, permits, recommendations, or any form granted to individuals, groups of people, or companies/foundations by government agencies outside the provisions of the applicable laws and regulations can be categorized as Gold Mining Without Permits (ASCGM). Considering that ASCGM activities do not apply mining principles correctly (good mining practice), this activity causes various negative impacts such as environmental damage and waste of non-renewable mineral resources (Rhani *et al.*, 2012). ASCGM activities are found in various places in Indonesia, one of which is in Sungai Jering Village, Pangkalan Jambu District, Merangin Regency, Jambi Province.

Waste of mineral resources occurs because only high-grade gold ore is extracted for processing by the traditional method of amalgamation. This method is carried out by binding the gold medal from the ore using mercury (Hg) in an amalgamator tube. This method causes a lot of gold medals to be wasted; this is reflected in the low level of gold metal recovery (<60%) and heavy metal mercury (Hg), which is wasted into the environment at significant levels (Widodo, 2011). As a result, problems arise from the method used, namely mercury contamination of the land and waters around the former gold mining area.

According to Sembel (2015), all forms of mercury are toxic. In the aquatic environment, inorganic mercury, namely Hg_2^{2+} and Hg^{2+} ions, is converted by microorganisms into methyl mercury which is very toxic and easily absorbed into the organism's tissues endangering the biota communities around the waters (Naswir *et al.*, 2020). Waters contaminated with mercury will endanger human health, including it can cause damage to the nervous system, itchy skin (irritation), genetic defects, and even death (Syidiq *et al.*, 2016). Mercury will enter through the food chain and accumulate in fish and river biota so that humans will experience poisoning if they consume fish and aquatic biota continuously for a long time.

The high toxic effect of mercury makes mercury decontamination efforts, especially in the former ASCGM land, very important. Several methods have been reported in efforts to decontaminate mercury, namely: coagulation (Syamsur *et al.*, 2018), filtration (Spiridonova *et al.*, 2020), adsorption (Ngatijo *et al.*, 2017). Coagulation is easy to do but often uses coagulants that are expensive and hard to obtain. Filtration is relatively easy and uses cheap but less efficient materials (Ngatijo *et al.*, 2019). Adsorption using cheap, highly available, and easy-to-use adsorbents is an effective method of decontaminating heavy metals such as mercury (Basuki *et al.*, 2018). Some of the adsorbents that have been reported in the decontamination of mercury are bentonite (Naswir *et al.*, 2020), activated charcoal waste from banana peels (Qadrini, 2020), agricultural waste and crop weeds (Zaki, 2017), water hyacinth fiber (Rikhanatul, 2018), and silica (Ngatijo *et al.*, 2017; Rabie *et al.*, 2019). The adsorbent does have the advantage that it is cheap and easy to obtain, but it is less efficient in post-absorption separation, primarily if it is carried out in a batch system.

Silica, which is synthesized from rice husk ash and then modified with ammonium and magnetite groups, is a suitable adsorbent for mercury adsorption because it comes from readily available material, inexpensive, and has easy application because it can be separated easily by magnetic withdrawal. Besides, silica gel is also reported to contain mercury-responsive silanol (Si-OH) and siloxane (Si-O-Si) functional groups, good stability, non-swelling, has high mass exchange, porosity, and surface area, and has a high resistance to heat (Ngatijo *et al.*, 2020a; Nuryono *et al.*, 2014). This research is motivated by the scarcity of studies on adsorbents that are easily separated after adsorption on mercury decontamination, especially in ex-mining soils. This study aims to synthesize quaternary ammonium silica functionalized magnetite (Fe_3O_4 / SAK) as an inexpensive, readily available adsorbent and is separated post adsorption in mercury decontamination from ASCGM soil samples. Furthermore, studies regarding the characterization and performance of Fe_3O_4 / SAK will be discussed in-depth in this article.

2. Material and Method

2.1. Material

Chemical agents include hydrochloric acid (HCl), sodium hydroxide (NaOH), 3-aminopropyltrimethoxysilane (3-APTMS), toluene, methyl iodide (CH_3I), sodium bicarbonate

($NaHCO_3$), iron (III), chloride hexahydrate ($FeCl_3.6H_2O$), iron (II) sulfate heptahydrate ($FeSO_4.7H_2O$), ammonium hydroxide (NH_4OH), nitric acid (HNO_3), mercury nitrate ($Hg2(NO_3)_2$) obtained from the manufacturer Merck® without further purification. Other supporting materials needed are Whatman 42 filter paper, universal indicators, and distilled water. Soil samples of mercury waste were taken from Sungai Jering Village, Pangkalan Jambu District, Merangin Regency, Jambi Province. The soil sampling location is 50 m from the ASCGM site at a depth of 0-10 cm from the ground. The soil sample is then put into an airtight plastic bag so that no chemical changes occur when analyzed. Rice husks are taken from rice mills around the Muaro Jambi area.

2.2 Instrument

Functional group analysis from Fe_3O_4/SAK performed using Fourier Transform Infrared (FTIR: Prestige 21) by mixing Fe3O4 / SAK powder with Kbr pellets and measured at a wavenumber 400-4000 cm-1. Crystallinity analysis was performed using X-Ray Diffraction (XRD: Bruker D2 Phaser) under operating conditions at 40 kV and 20 mA with radiationbCuKα (λ=1,5404 Å) and the goniometer speed of 0,6°2θ/ minutes at intervals 0,01° at an angle 2θ=5-60°. Analysis of surface morphology and constituent elements Fe_3O_4/SAK was performed using Scanning Electron Microscopy-Electron Dispersive X-Ray (SEM-EDX; Phenom Desktop ProXL) at a magnification of 5000 ×. Surface area analysis Fe_3O_4/SAK performed with a Surface Area Analyzer (SAA: Quantachrome Novatouch Lx4) using liquid nitrogen at 77,035 K; Data analysis used the Brunauer Emmet Teller (BET) equation to obtain data on the surface area, pore radius, and total pore volume. Quantitative analysis of mercury was carried out with a mercury analyzer (Lab Analyzer 254) with the ISO / IEC-17025-2005 testing standard using a cold vapor atomic absorption spectrophotometer (CV-AAS). A set of glass support equipment (Erlenmeyer, beaker, funnel), oven, furnace, analytical balance, burette and stative, pH meter, reflux device, hot plate stirrer, and shaker were also used in this study.

2.3 Fe_3O_4/SAK Synthesis

Fe3O4/SAK synthesis was carried out based on previous research procedures (Ngatijo *et al.*, 2020a) begins with the destruction of silicic acid from rice husk ash (ASP). The rice husks were burned to become ASP, then the ASP was burned at 700˚C for 3 hours, after which it was crushed and sieved at 200 mesh size. A total of 60 grams of ASP was added to 80 grams of NaOH crystals and 500 mL of distilled water, then heated and stirred for 3 hours. The suspension is then cooled and filtered. A total of 200 mL of filtrate from the red filter was added with 4M HCl solution dropwise to a pH of 9, left for 3 × 24 hours to form a gel. The gel that is formed is then washed to a neutral pH, filtered, dried in an oven at a temperature of 70 menghasilkanC and crushed to produce silica gel powder (SG).

A total of 12 grams of SG, 10 mL 3-APTMS, 20 mL toluene, and 10 mL of methyl iodide are added to a three-neck flask then refluxed for 6 hours at 100˚C while 10 mL of methyl iodide are added dropwise in a dark room. The precipitate that is formed is then washed with a solution of NaHCO3 and distilled water. The precipitate was dried at 70˚C and crushed to obtain quaternary ammonium silica (SAK).

A total of 1 gram of magnetite, Fe3O4 based on the preparation results from Ngatijo, Bemis, *et al.*, (2020) and Rusdiarso *et al.*, (2020) which is still fresh, is dissolved in 2 mL HCl—then mixed with 10 mL of SAK solution dissolved in 10 mL of ethanol. The solution was then neutralized by adding 0.1 M NaCl / 0.1 M HCl. The solution was heated at 80˚C and stirred for 45 minutes. The precipitate formed is then separated with an external magnet and rinsed with distilled water until a neutral pH. The precipitate is then dried at 70˚C and crushed as Fe3O4 / SAK.

2.3.1 Decontamination of Mercury from Artificial Waste and Ex-Mining Soil

The mercury decontamination process is carried out based on the adsorption principle using a batch reactor type (Ngatijo *et al.*, 2019). The process begins with optimizing the adsorption conditions, namely, optimizing the adsorbent's pH and mass. Optimization of the adsorption pH was carried out with as many as five Erlenmeyer, each containing 20 mL of Hg22 + 10 ppm ion solution, which had been adjusted to pH 3, 4, 5, 6, and 8 with the addition of HNO3 or NaOH interacted with 0.1 gram of Fe3O4/SAK adsorbent. . The mixture was then stirred for 30 minutes. Next, the mixture is separated with an external magnet and filtered with filter paper. The filtrate obtained was analyzed for the Hg22 + ion content with a mercury analyzer instrument. The effect of the variation of the adsorbent mass was carried out with five Erlenmeyer, each containing 20 mL of Hg22 + 10 ppm ionic solution, which had been adjusted to the optimum pH and interacted with the Fe3O4 / SAK adsorbent with a variation of the adsorbent mass, namely 0.05; 0.1; 0.15; 0.2; and 0.25 g. The mixture was then stirred for 30 minutes. Next, the mixture is separated with an external magnet and filtered with filter paper. The filtrate obtained was analyzed for the Hg22 + ion content with a mercury analyzer instrument.

Mercury decontamination from ex-mining soil begins with scouring and sieving the soil, then dissolving 1 gram of soil in aquaria solution, namely HNO3: HCl (1: 3) to dissolve mercury in the soil. The mercury content in the soil sample is the total content of the metal ions Hg22 + and Hg2 +. The solution was then diluted ten dilutions and allowed to stand for 3 × 24 hours. The solution is then filtered and adjusted to the optimum pH. A total of 20 mL of the soil solution then interacts with 0.1 g of Fe3O4 / SAK adsorbent for 30 minutes. The mixture is then separated with an external magnet. The solutions before and after the adsorption process were analyzed using a mercury analyzer instrument.

3. Result and Discussion

3.1. Fe_3O_4/SAK Characteristic

Synthesis of Fe_3O_4/SAK carried out in 4 stages, namely the synthesis of silica gel (SG) from rice husk ash, the formation of Promer amine silica (SAP), the formation of SAK, and the functionalization of magnetite with SAK. Synthesis of the SMAK coated Fe3O4 adsorbent was started from the ashing stage of the rice husks. Rice husks were burned in a furnace at 700˚C for 3 hours to obtain rice husk ash (ASP) (Reaction Equation 1). Silica gel (SG) was obtained from alkaline extraction (digestion) by the sol-gel method. In the alkaline extraction stage, 4M NaOH was used to dissolve 60 grams of ASP, then heated at 60-70˚C and stirred for 3 hours until the solution became thick black. The thick black solution is filtered to obtain a brownish-red filtrate which is Na2SiO3 (sodium silicate) (Reaction Equation 2). The sodium silicate solution obtained is used as a precursor in the sol-gel process. The sol-gel process is carried out by adding a dropwise 4M HCl solution until pH 9 is reached to obtain silicic acid or silica hydrosol (H2SiO3), an insoluble stable gel (Eq. 3).

$$\text{Senyawa C, H, dan Si)}_{(s)} + 3O_{2(g)} \rightarrow CO_{(2)(g)} + 2H_2O_{(g)} + SiO_{2(s)} \quad (1)$$

$$SiO_{2(s)} + 2NaOH_{(aq)} \rightarrow Na_2SiO_{3(aq)} + H_2O_{(l)} \quad (2)$$

$$Na_2SiO_{3(aq)} + 2HCl_{(aq)} \rightarrow H_2SiO_{3(s)} + 2NaCl_{(aq)} \quad (3)$$

Gel formation was left for 3 × 24 hours so that the gel was obtained optimally. The formed gel was filtered and washed with distilled water to remove Na ions, metal oxides and excess acid and dried in an oven at 70˚C to obtain a white silica gel (SG) powder. The Si-OH group, which dominates the surface of the silica gel, reacts rapidly with organosilanes compounds (Cestari *et al.*, 2000), so that it can be modified with a 3-APTMS compound (Aminopropyltrimethoxysilane) which has an amine group (R-NH2). Modifications were made through the grafting method. The amine group in SAP is then converted into a positively charged quaternary ammonium group [(-N + (CH3) 3] through a methylation reaction by reacting SAP with alkyl halides under alkaline conditions through the Nucleophilic Substitution reaction mechanism-2 (SN2). The hypothetical reaction mechanism for the formation of SAK is presented in Figure 1.

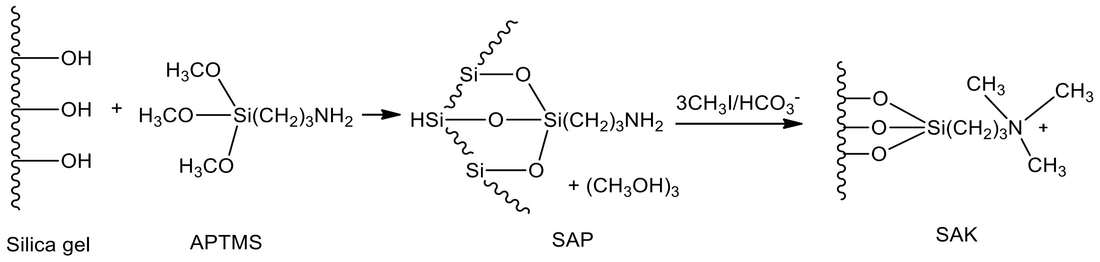

Figure 1. Hipotetic mechanisms of SAK formation reaction

The functionalization of magnetite with SAP was carried out by dissolving 1 gram of Fe3O4 with 2 mL of HCl. This acidification aims to form the active site on the Fe3O4 surface; that is, the O^- bound to the Fe atom will experience protonation due to H + from the HCl solution so that the active side formed will be more easily reached with the siloxy group ($^-$O-Si≡) of the silicate anion. on SAK. The free electrons from the ($^-$O-Si≡) group will attack the Fe atom to obtain the Fe-O-Si bond. The hypothetical mechanism of the magnetite functionalization reaction by SAK is shown in Figure 2.

The functional group characterization results (FT-IR) as an indication of the success of the Fe3O4 / SAK synthesis process are shown in Figure 3A. The FTIR SG and SAK spectra indicated the presence of silanol (Si-OH) and siloxane (Si-O-Si) groups. The absorption band that appears in the wavenumber range 3700-3200 cm-1 indicates a stretching vibration of the hydroxyl group (–OH) from Si-OH; this is in accordance with the presence of broadband found at wave number 3366 cm^{-1} (Silverstein *et al*., 2005). The absorption at wave number 1636 cm-1 shows the absorption band of the -OH group bending vibrations on Si-OH (Nuryono *et al*., 2014). The asymmetric stretching vibration of Si-O in Si-O-Si is indicated by the presence of a solid and sharp absorption band at wavenumbers 1046 cm-1 and 953 cm-1, respectively, showing stretching vibrations of the Si-O groups on Si-OH (Mujiyanti *et al*., 2010). This result is also in accordance with the literature that the wavenumber 1110-830 cm-1 is an absorption band showing Si-O (Silverstein *et al*., 2005). At wave number 780 cm^{-1}, an absorption band appears, showing the stretching vibration of Si-O SYMMETRY on Si-O-Si. (Buhani *et al*., 2009), At the wave number 441.61 cm-1, the absorption band of the Si-O bending vibration in Si-O-Si (Widjonarko *et al*., 2014).

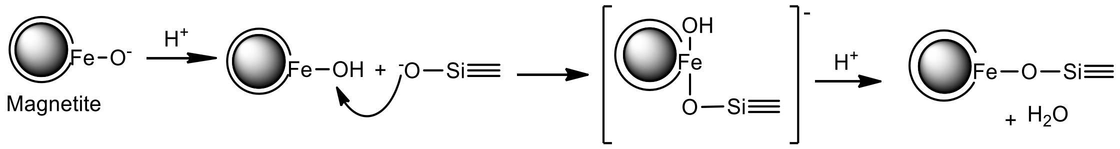

Figure 2. Magnetite fuctionalization reaction by SAK

The success of magnetite functionalization with SAK is shown in the emergence of a new absorption band at wave number 544 cm-1, indicating the presence of Fe-O stretching vibrations in Fe-O-Si (Lin *et al*., 2011). The new absorption band indicates that SAK has successfully coated Fe3O4. The wavenumber 3368 cm-1 shows a stretching vibration of –OH from Si-OH and a bending vibration of –OH, shown at wave number 1636 cm^{-1}. The absorption bands that appear at wavenumbers 2938 cm-1 and 2851 cm^{-1} show the stretching vibrations of CH from CH2 and CH3, at wavenumbers 1065 cm^{-1} appear strong and sharp absorption bands showing Si-O vibrations from Si -O-Si. The absorption band at wave number 955.23 cm^{-1} shows the Si-O vibration from Si-OH, then at wave number 795 cm^{-1} shows the Si-O symmetric stretching vibration from Si-O-Si at wave number 449 cm-1 shows the Si-O buckling vibration of Si-OS. The success of Fe3O4-SAK adsorbent synthesis is indicated by the presence of distinctive absorption bands that indicate Si-OH, Si-O-Si, C-H, and Fe-O-Si.

(A) **(B)**

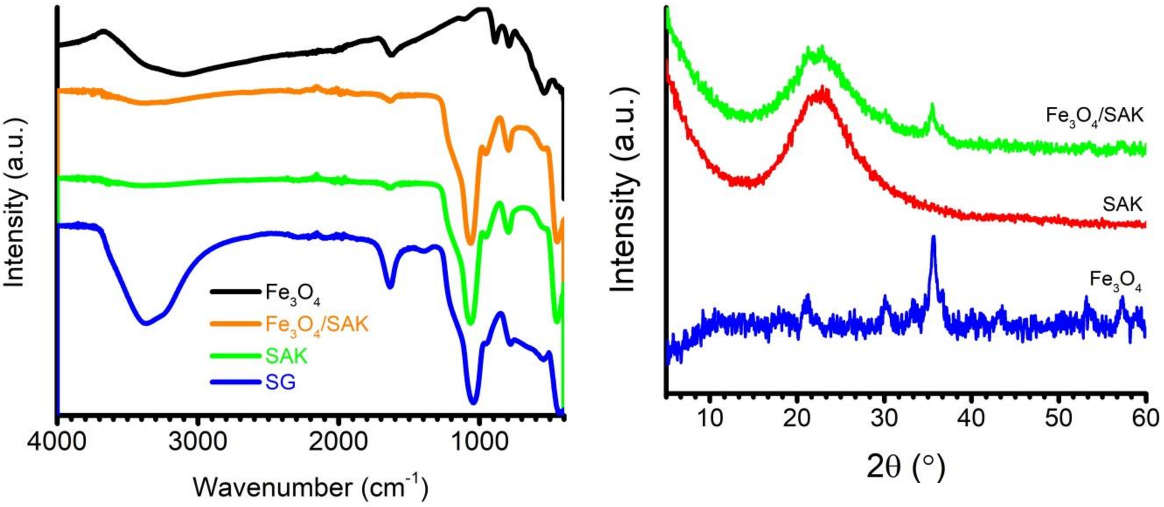

Figure 3. (A) FT-IR spectra of SG, SAK, Fe_3O_4, and Fe_3O_4/SAK, dan (B) XRD diffractogram of SAK, Fe_3O_4, dan Fe_3O_4/SAK.

The XRD SAK diffraction pattern (Figure 3B) shows a typical high-intensity peak of silica at an angle 2θ 22,96˚. This result is following the research from Kalapathy *et al.*, (2003) that the typical peak of SiO2 is around the angle of 2θ = 20-25˚. The diffraction pattern has an irregular structure, indicating that SAK's crystal structure is amorphous (Buhani *et al.*, 2009). The Fe3O4 diffractogram shows the typical peaks of Fe3O4 especially at an angle of 2θ, namely 18.45˚; 30.35˚; 35.70˚; 53.62˚ and 57.32 according to JCPDS data No. 00-033-0664 (Ngatijo *et al.*, 2020). The highest intensity is obtained at 2θ = 35.70˚. This suitability indicates that the synthesis of Fe3O4 has been successfully carried out. Fe3O4 / SAK synthesis's success is indicated by the appearance of the diffraction peaks of Fe3O4 and SiO2. The Fe3O4 coating process with SMAK relatively does not change the diffraction pattern of Fe3O4 but changes the intensity at 2θ = 35.52˚, which is the diffraction peak with the highest intensity of typical Fe3O4 peaks having a lower intensity than the diffraction peak of Fe3O4.

SEM-EDX aims to see the surface morphology and elemental composition of the adsorbent that has been synthesized. The results of SEM characterization with a magnification of 5000 times showed changes in surface morphology from the synthesis of each material (Figure 4). It appears that SAK has a smoother surface, amorphous structure, contains particle clusters, evenly distributed (homogeneous) particles, and has quite a lot of pore cavities. The surface morphology of Fe3O4 has non-uniform particle shapes, which are generally round and pointed (Zhang *et al.*, 2013). The elemental composition analysis using EDX shows that Si and O elements have the highest content, namely 50.51% and 44.20%, respectively, in SAK material. Fe3O4-SMAK contains Si and O as much as 44, 74%, and 43.32%, indicating that the adsorbent contained SiO2 compounds. Then element C is found in SMAK and Fe3O4-SMAK, respectively, indicating a quaternary group in both materials. The Fe element in the synthesis of Fe3O4 contains as much as 68.44% and O element as much as 24.14%. In the elemental composition of the Fe3O4-SMAK adsorbent, there is also an element of Fe which has a content of 3.92%. Elemental composition analysis using EDX shows that Si and O elements have the highest content, namely 50.51% and 44.20%, respectively. SAK material, then in the elemental composition of Fe3O4-SMAK, contains elements of Si and O that contain 44.74% and 43.32%, which indicates that the adsorbent contains SiO2 compounds. Then element C is found in SMAK and Fe3O4-SMAK, respectively, indicating a quaternary group in both materials. The Fe element in the synthesis of Fe3O4 contains as much as 68.44% and O element as much as 24.14%. In the elemental composition of the Fe3O4-SMAK adsorbent, there is also an element of Fe which has a content of 3.92%.

(A) **(B)** **(C)**

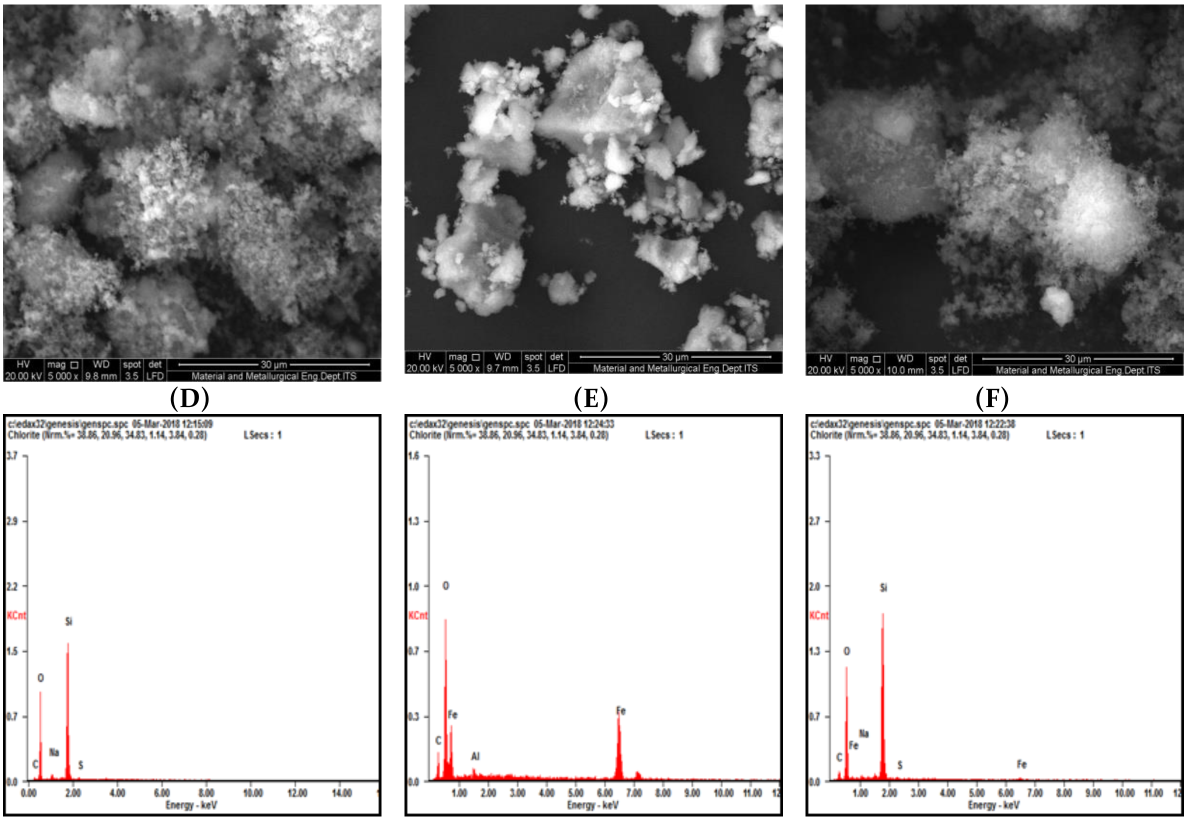

(D) (E) (F)

Figure 4. SEM image and elemental composition analysis of SAK (A & D), Fe$_3$O$_4$ (B & E), dan Fe$_3$O$_4$/SAK (C & F).

Surface area, particle size, and pore diameter are essential characteristics for adsorbents. Adsorbent which has a small particle size, namely nanoparticles (1-100 nm) has a large surface area and pore diameter, this will increase the adsorption capacity because the adsorbent absorbs more adsorbate. The SAA analysis results on Fe3O4 / SAK have a surface area of 224,984 m2 / g; this is following the specific surface area of the adsorbent, namely 100-1000 m2 / g. Previous studies reported that silica gel and silica modified with -NH2 groups had surface areas of 95.77 m2 / g and 130.65 m2 / g, respectively (Nuryono *et al*., 2014). These results indicate that the functionalization of magnetite with FAS increases the surface area. The measured particle diameter of Fe3O4 / SAK was 7.82 nm and was included in the mesoporous category.

3.2 Dekontaminasi Merkuri

pH greatly affects the adsorption capacity of an adsorbent because the activity of functional groups on the adsorbent surface can change and affect the solubility of metal ions as the adsorbate. The pH variations used in this study were 3, 4, 5, 6, and 8. These pH variations are based on the distribution of the Hg22 + solubility specimen at various pHs according to the pourbaix diagram. According to (Zhou, 2013) the solubility of Hg$_2^{2+}$ metal ions is primarily stable at pH 1-5. In the pH range, 6-14, the stability decreases due to the increase in Hg$_2$(OH)$_2$ species so that the solubility of Hg$_2^{2+}$ ions decreases and becomes a yellowish precipitate. Mercury ion (I) or also called mercury, unlike other monovalent metal cations such as copper (I) ions, mercury (I) ions exist in the form of Hg22 + in solution. This fact happened because mercury (I) ions tend to form covalent bonds instead of ionic bonds to form Hg + -Hg + (Roesmer and Kruger, 1960). The effect of pH variation on adsorption efficiency has high efficiency of 99.94%, and the most excellent efficiency is almost 100%, namely 99.99% at pH 4. This fact indicates that the Fe3O4-SMAK adsorbent synthesized is very effective for adsorbing Hg22 + metal ions. The adsorption efficiency increased at pH 3 to 4, then there was a significant decrease in efficiency at pH 5-8 (Figure 5A). This result is following the statement (Zhou, 2013) that the OH$^-$ ion will increase at higher pH so that the Hg22 +

species in the solution decreases, and a precipitate occurs. It will change to the Hg2 (OH) 2 species in an alkaline state, which is a yellowish solid.

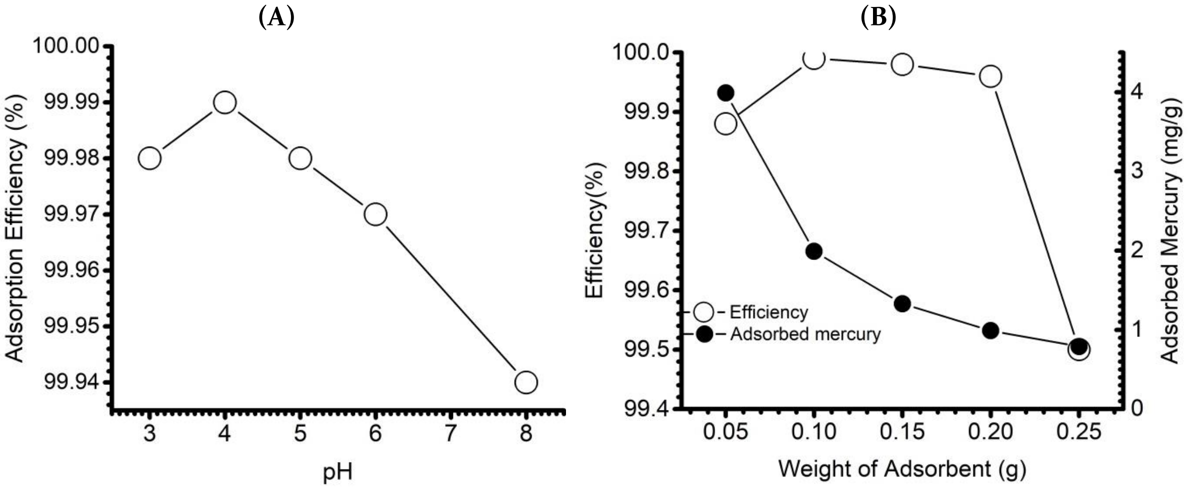

Figure 5. (A) Adsorption efficiency as function of pH; (B) Effect of adsorbent weight to efficiency (%) and adsorbed mercury (mg/g)

The adsorbent mass is one of the adsorption parameters, namely, the more the mass of the adsorbent used, the more adsorbate is absorbed so that the adsorption efficiency will also increase and achieve equilibrium. Based on the graph obtained in Figure 5B, it can be seen that the adsorption efficiency has increased in the adsorbent mass from 0.05 to 0.1 grams. This is consistent with the statement that the more adsorbent, the more adsorbate will be absorbed. The adsorption efficiency obtained from the adsorbent mass variation was high and fast (contact time was 30 minutes). At the adsorbent mass of 0.1 gram, the most outstanding adsorption efficiency was achieved to absorb mercury, namely 99.99%. The adsorption efficiency began to decline when the adsorbent mass increased, namely at 0.15-0.25 grams. A drastic decrease occurred in the adsorbent mass of 0.25 grams and had the lowest adsorption efficiency of 99.50%. The same trend was also reported by Aulia and Effendi (2020) where after passing the optimum mass of adsorbent (10 g), the adsorption of mercury tends to decrease. The increase in adsorbent mass should increase the amount of mercury adsorbed because the adsorbent's active site increases. However, after passing the optimum mass, the more adsorbent, the less adsorbed mercury. The possible explanation is due to the equilibrium of the Hg22 + metal ions in the solution. As described by Ningsih *et al.* (2016), Abundant active sites (large adsorbent mass) will make the rate of desorption (the release of adsorbate from the adsorbent back into solution) is greater, and the adsorbed mercury decreases.

Based on the research results, the Fe3O4-SMAK adsorbent that has been synthesized can absorb mercury metal, so the adsorbent is applied to adsorb mercury metal found in soil samples. The sample came from Sungai Jering Village, Pangkalan Jambu District, Merangin Regency, Jambi Province, the former gold mining area. As it is well known, mercury metal is one of the wastes produced by ASCGM (Gold Mining Without Permits) activities and will have a dangerous impact on humans and the surrounding environment.

Table 1. Analysis result of the mercury level of soil samples before and after adsorption decontamination

Sample	$C_{initial}$ (ppm)	C_{final}(ppm)	Amount of adsorbed mercury ions (ppm)	Adsorption Efficiency (%)
Soil	0.1665	0.0943	0.0722	43.36

The results of the comparison of the mercury content in soil samples that have been dissolved before and after adsorption at optimum pH 4.0 are shown in Table 1.Based on the analysis results in Table 1; it can be seen that the Fe_3O_4 / SAK adsorbent can absorb mercury content in the soil, which can be seen from the adsorption efficiency. obtained by 43.36% (0.722 mg / g). This shows that the synthesized adsorbent can be applied as an adsorbent that is easily separated after mercury decontamination in the former gold mining area. The mercury decontamination capacity of this study is relatively high when compared to previous studies with different adsorbents on artificial mercury samples: 0.45 mg / g of mercury in activated charcoal from kapok banana waste (Qadrini, 2020), 38 mg / g of mercury in amine-modified silica nanoparticles (Rabie *et al.*, 2019), and 0.299 mg / g mercury on agricultural waste and weed adsorbents (Zaki, 2017).

4. Conclusions

Mercury decontamination is a necessary process given the prevalence of ASCGM, particularly in Jambi Province. This study succeeded in synthesizing Fe_3O_4 / SAK adsorbent, which was characterized by the siloxane, silanol, methylene, and Fe-O (FTIR) functional groups and the emergence of typical peaks of SiO_2 and Fe_3O_4, namely at 2θ 22.88° and 35.52, respectively. ° (XRD). SEM-EDX characterization results showed that SAK successfully coated Fe_3O_4 from the surface morphology and composition of the main elements obtained, namely C, O, Si, and Fe. SAA characterization results showed that the surface area and pore diameters were 224.984 m2 / g and 36.149-38.70 Å, respectively. The optimum results for adsorbing Hg22 + metal ions were obtained at pH 4, and the mass of the adsorbent Fe_3O_4 / SAK was 0.1 gram. Fe_3O_4 / SAK adsorbent has been proven to be used as an adsorbent that is easily separated after adsorption on decontamination of mercury from ex-mining soil samples with an adsorption efficiency of 43.36% (0.722 mg / g).

Acknowledgment

The author would like to thank the Ministry of Education and Culture-Dikti and Jambi University for funding this research through the Higher Education Leading Applied Research (PT-UPT) scheme with No. contract: 2653 / UN21.18 / PG / SPK / 2020.

Reference

Aulia, R.R., Effendi, A.J., 2020. Penyisihan Merkuri (Hg) dari Air Hasil Pencucian Tanah Menggunakan Adsorben GAC Terimpregnasi Fe Dan Ce. Jurnal Teknik Lingkungan. 26, 37–52.

Basuki, R., Ngatijo, Santosa, S.J., Rusdiarso, B., 2018. Comparison the new kinetics equation of noncompetitive sorption Cd(II) and Zn(II) onto green sorbent horse dung humic acid (HD-HA). Bull. Chemical Reaction Engineering *& Catalysis*. 13, 475–488.

Buhani, B., Narsito, N., Nuryono, N., Kunarti, E.S., 2009. Amino and mercapto-silica hybrid for Cd (II) adsorption in aqueous solution. Indonesian Journal of Chemistry. 9, 170–176.

Cestari, A.R., Vieira, E.F.S., de A Simoni, J., Airoldi, C., 2000. Thermochemical investigation on the adsorption of some divalent cations on modified silicas obtained from sol--gel process. Thermochim. Acta 348, 25–31.

Kalapathy, U., Proctor, A., Shultz, J., 2003. Silicate thermal insulation material from rice hull ash. *Industrial* & *Engineering Chemistry Research*. 42, 46–49.

Lin, Y., Chen, H., Lin, K., Chen, B., Chiou, C., 2011. Application of magnetic particles modified with amino groups to adsorb copper ions in aqueous solution. Journal of Environmental Science. *23, 44–50.*

Mujiyanti, D.R., Nuryono, N., Kunarti, E.S., 2010. Sintesis dan karakterisasi silika gel dari abu sekam padi yang diimobilisasi dengan 3-(trimetoksisilil)-1-propantiol. Journal of Sains and Terapan Kimia. 4, 150–167.

Naswir, M., Desfaurnatalia, Y., Septiarini, L., Gusti Wibowo, Y., 2019. Activated Bentonite: Low Cost Adsorbent to Reduce Mercury Content in A Solution. Research Journal of Applied Sciences. 14, 243–249.

Naswir, M., Natalia, D., Arita, S., Wibowo, Y.G., 2020. Adsorption of Mercury Using Different Types of Activated Bentonite : A Study of Sorption , Kinetics , and Isotherm Models. Journal *of* Environmental Chemical Engineering. *15, 1*23–131.

Ngatijo, N., Basuki, R., Nuryono, N., Rusdiarso, B., 2019. Comparison of Au(III) Sorption on Amine-Modified Silica (AMS) and Quaternary Amine-Modified Silica (QAMS): A Thermodynamic and Kinetics Study. Indonesian Journal of Chemistry. 19, 337–346.

Ngatijo, N., Basuki, R., Rusdiarso, B., Nuryono, N., 2020a. Sorption-desorption profile of Au (III) onto silica modified quaternary amines (SMQA) in gold mining effluent.Journal of Environmental Chemical Engineering. *8, 103747.*

Ngatijo, N., Bemis, R., Aziz, A., Basuki, R., 2020b. Reinforcement of Quaternary Ammonium Modified Silica (QAMS) with Magnetite and its Application by Solid Phase Adsorption (SPA) to Adsorb Chromate Ions. Jurnal *Kimia* Sains *dan Aplikasi*. 23, 338–345.

Ngatijo, N., Nuryono, N., Faried, F., Batubara, U.M., Ula, S.M., Sari, I.P., 2017. Pembuatan Lahan Percontohan Tanaman Padi (Oriza Sativa L.) melalui Recovery Logam Berat. CHEMPUBLISH J. 2, 1–10.

Ningsih, D.A., Said, I., Ningsih, P., 2016. Adsorpsi logam timbal (Pb) dari larutannya dengan menggunakan adsorben dari tongkol jagung. Jurnal *Akademika Kimia.* 5, 55–60.

Nuryono, N., Rosiati, N.M., Rusdiarso, B., Sakti, S.C.W., Tanaka, S., 2014. Coating of magnetite with mercapto modified rice hull ash silica in a one-pot process. Springerplus. 3, 515.

Qadrini, L., 2020. Penyerapan Ion Logam Merkuri Menggunakan Arang Aktif Limbah Kulit Pisang Kepok (Musa paradisiaca Formatypica). KOVALEN Journal Reserch of Chemist. 6, 39–44.

Rabie, A.M., Abd El-Salam, H.M., Betiha, M.A., El-Maghrabi, H.H., Aman, D., 2019. Mercury removal from aqueous solution via functionalized mesoporous silica nanoparticles with the amine compound. Egypt. Jurnal. Pet. 28, 289–296.

Rhani, H.C., others, 2012. Faktor Faktor yang Berhubungan dengan Kadar Merkuri (Hg) pada Tanah Pemukiman Warga di Sekitar Lokasi Penambangan Emas Tradisional (Studi Kasus di Desa Jendi, Kecamatan Selogiri, Kabupaten Wonogiri, Provinsi Jawa Tengah). Jurnal Kesehatan Masyarakat Universitas Diponegoro. 1, 18738.

Rikhanatul, F.P., 2018. Penurunan Logam Hg Dalam Air Dengan Kombinasi Adsorpsi dan Fitoremediasi Menggunakan Biosorben Serat Eceng Gondok (Eichhornia crassipes) Dan Tanaman Melati Air (Echinodorus palaefolius) Di Dalam Sistem Sub-Surface Flow Constructed Wetland. Universitas Gadjah Mada.

Roesmer, J., Kruger, P., 1960. The radiochemistry of mercury. Research Org.: Nuclear Science and Engineering Corp.

Rusdiarso, B., Basuki, R., 2020. Stability Improvement of Humic Acid as Sorbent through Magnetite and Chitin Modification. Jurnal Kimia Sains dan Aplikasi. 23, 152–159.

Sembel, D.T., 2015. Toksikologi Lingkungan Dampak Pencemaran dari Berbagai Bahan Kimia dalam Kehidupan Sehari-hari. Yogyakarta Andi.

Silverstein, R.M., Webster, F.X., Kiemle, D.J., 2005. Proton NMR spectrometry. Spectrom. Identif. Org. Compd. 7th ed.; John Wiley Sons Inc. New York, NY, USA 142.

Spiridonova, T., Mardjan, M., Ridha, A., 2020. Perbandingan Efektivitas Zeolit dan Karbon Aktif dalam Menurunkan Kadar Merkuri (Hg) dengan Metode Penyaringan pada Air Sungai Mandor. JUMANTIK Jurnal Mahasiswa dan Peneliti Kesehatan. 6, 50–58.

Syamsur, N.N., Ihsan, I., Sahara, S., 2018. Pengolahan Limbah Cair Laboratorium Kimia dengan Menggunakan Metode Elektrokoagulasi dan Koagulan Biji Kelor. JFT Jurnal Fisika dan Terapan. 5, 119–127.

Syidiq, A.B., Amiruddin, A., Sirih, H.M., 2016. Jenis Penyakit Yang Diderita Penambang Emas Tradisional Pada Daerah Aliran Sungai Watu-Watudi Kecamatan Lantari Jayakabupaten Bombana. AMPIBI J. Alumni Pendidik. Biol. 1, 65–70.

Widjonarko, D.M., Jumina, J., Kartini, I., Nuryono, N., 2014. Phosphonate Modified Silica for Adsorption of Co (II), Ni (II), Cu (II), and Zn (II). Indones. Journal of Chemist. 14, 143–151.

Widodo, A., 2011. Upaya Perolehan Emas dengan Metode Amalgamasi Tidak Langsung. Studi Kasus

Pertambangan Rakyat Desa Waluran Kecamatan Waluran Kabupaten Sukabumi. Bulletin *of Environmental* Geology. 21, 83–96.

Winarno, T., Ali, R.K., Langit, W.R., 2020. Potensi Pembentukan Air Asam Tambang Pada PIT 3000, Blok Toraja, PT Trubaindo Coal Mining Berdasarkan Studi Karakteristik Geokimia dan Mineralogi Batuan Overburden dan Underburden. *Jurnal* Presipitasi *:* Media Komunikasi dan Pengembangan Teknik Lingkungan. 17, 52–61.

Zaki, M., 2017. Penyisihan Ion Logam Merkuri (Hg2+) menggunakan Adsorben Berbahan Baku Limbah Pertanian dan Gulma Tanaman. Journal Teknik Kimia. USU 6, 7–11.

Zhang, X., Zhang, P., Wu, Z., Zhang, L., Zeng, G., Zhou, C., 2013. Adsorption of methylene blue onto humic acid-coated Fe3O4 nanoparticles. Colloids *and* Surfaces A: Physicochemical and Engineering. 435, 85–90.

Zhou, Z., 2013. Mercury stabilization using thiosulfate or selenosulfate (Doctoral Dissertation). University of British Columbia.